Molecular phylogeny and node time estimation of bioluminescent Lantern Sharks (Elasmobranchii: Etmopteridae)

Nicolas Straube [a,*], Samuel P. Iglésias [c], Daniel Y. Sellos [c], Jürgen Kriwet [b], Ulrich K. Schliewen [a]

[a] Zoologische Staatssammlung München, Sektion Ichthyologie, Münchhausenstraße 21, 81247 München, Germany
[b] Staatliches Museum für Naturkunde Stuttgart, Sektion Paläontologie, Rosenstein 1, 70191 Stuttgart, Germany
[c] Muséum national d'Histoire naturelle, Département Milieux et Peuplements aquatiques, USM 0405, Station de Biologie Marine de Concarneau and UMR 7208 CNRS/MNHN/IRD/ UPMC, Biologie des Organismes et Ecosystèmes Aquatiques, 29182 Concarneau cedex, France

ARTICLE INFO

ABSTRACT

Deep-sea Lantern Sharks (Etmopteridae) represent the most speciose family within Dogfish Sharks (Squaliformes). We compiled an extensive DNA dataset to estimate the first molecular phylogeny of the family and to provide node age estimates for the origin and diversification for this enigmatic group. Phylogenetic inferences yielded consistent and well supported hypotheses based on 4685 bp of both nuclear (RAG1) and mitochondrial genes (COI, 12S-partial 16S, tRNAVal and tRNAPhe). The monophyletic family Etmopteridae originated in the early Paleocene around the C/T boundary, and split further into four morphologically distinct lineages supporting three of the four extant genera. The exception is *Etmopterus* which is paraphyletic with respect to *Miroscyllium*. Subsequent rapid radiation within *Etmopterus* in the Oligocene/early Miocene was accompanied by divergent evolution of bioluminescent flank markings which morphologically characterize the four lineages. Higher squaliform interrelationships could not be satisfactorily identified, but convergent evolution of bioluminescence in Dalatiidae and Etmopteridae is supported.

1. Introduction

Lantern Sharks (Etmopteridae) are a highly diverse family of poorly known bioluminescent deep-sea elasmobranchs with 43 species in five genera (Compagno et al., 2005; Schaaf da Silva and Ebert, 2006). Although they represent the largest family of Squaliformes or Dogfish Sharks, it is one of the least studied among the order and very few data on their biology, life history, conservation and phylogenetics have been gathered. Etmopterids are rather small sharks including the smallest known shark, *Etmopterus perryi* (20 cm). The largest member *Centroscyllium fabricii* reaches a total length of 107 cm. Members of the family are distributed panoceanic in depths between 50 and 4500 m at slope regions. Their body is more or less densely covered with etmopterid specific hook-like or conical dermal denticles. Quite a few species had been known only from few specimens, but increased deep-sea fisheries recently yielded additional specimens of some rare species as well as from several undescribed species highlighting both the diversity of the family as well as the vulnerability of these longliving and slowly reproducing ovoviviparous sharks, which give birth to only 6–14 pups per litter (Compagno et al., 2005). Most detailed biological studies that have been published until now concentrate on a single Atlantic species, *Etmopterus spinax* (Claes and Mallefet, 2008, 2009; Coelho and Erzini, 2008a,b; Klimpel et al., 2003; Neiva et al., 2006).

Bioluminescence is a wide-spread phenomenon among inhabitants of the subphotic zone, but its occurrence is limited among sharks to only two squaliform families, the Dalatiidae and Etmopteridae. Photophores of etmoperids are concentrated on the dark ventral region and on more or less prominent and often species specific dark flank and tail markings. Claes and Mallefet (2008) suggest a function of camouflage by counter illumination for the numerous ventral photophores in *E. spinax*. Further studies suggest the elaborate flank and tail markings to function for intraspecific signalling i.e. as schooling aid (e.g. Reif, 1985; Claes and Mallefet, 2009).

The fossil record of Etmopteridae is comparatively poor and the phylogenetic assignment of extinct species is often difficult. The reason is, that articulated fossils of etmopterids are unknown so far and fossilized single teeth represent the only direct window of information to their past. The unambiguously oldest fossil teeth of Etmopteridae are known from the Eocene (Lutetian 48.6–40.4 Ma) and strongly resemble those of extant species (Adnet, 2006; Adnet et al., 2008; Cappetta and Adnet, 2001; Cigala, 1986; Ledoux, 1972). Fossils such as *Eoetmopterus* (Müller and Schöllmann, 1989), *Proetmopterus* (Siverson, 1993) and *Microetmopterus*

* Corresponding author. Fax: +49(0)898107300.
E-mail addresses: straube@zsm.mwn.de (N. Straube), Iglesias@mnhn.fr (S.P. Iglésias), sellos@mnhn.fr (D.Y. Sellos), kriwet.smns@naturkundemuseum-bw.de (J. Kriwet), schliewn@zsm.mwn.de (U.K. Schliewen).

(Siverson, 1993) have been assigned to Etmopteridae based on their tooth morphology, but nevertheless show only minor or very generalized similarities, respectively, to extant species' tooth morphologies. These species apparently went extinct by the end of the Cretaceous (Adnet et al., 2006). Their former habitat is debated, but interestingly they may not have been inhabitants of the bathyal environment adopted by extant species of Etmopteridae (Adnet et al., 2006). Therefore, and because the systematic assignment of these extinct species is not soundly demonstrated, the phylogenetic position of the latter within Squaliformes and especially their unambiguous assignment to Etmoperidae remains to be tested.

Not only the limitation of the fossil record to teeth, but also the low density of phylogenetically informative morphological characters (including tooth characters) have prevented a detailed phylogenetic investigation of the family. Additional practical limitations have arisen due to the scarcity of specimens available, which renders sampling efforts extremely difficult, e.g. availability of *Trigonognathus*.

Alternative characteristic dentition types of Etmopteridae have helped diagnosing genera rather than elucidating inter- and intrageneric phylogenetic relationships. Dentitions in etmopterids include a wide array of types. *Etmopterus* and juvenile *Miroscyllium sheikoi* are characterized by a "cutting–clutching type", whereas the dentition of *Centroscyllium, Aculeola* and adult *Miroscyllium sheikoi* is of the "clutching type". The "tearing type" dentition within etmopterids is restricted to *Trigonognathus* (Adnet et al., 2006). These unique types of dentition also allow identification of extinct Etmopteridae to genus level but provide little or often ambiguous information for species identification due to ontogenetic and sexual dimorphisms (Straube et al., 2008). Consequently, identification, classification and partially phylogenetics of the most speciose Lantern Shark genus *Etmopterus* (approx. 32 species (Compagno et al., 2005)) are based mainly on the shape of flank markings and the arrangement and shape of placoid scales (e.g. Compagno et al., 2005; Last et al., 2002; Schaaf da Silva and Ebert, 2006; Shirai and Nakaya, 1990a). Their characterists diagnose several species groups within the genus, i.e. (1) the "*Etmopterus lucifer* group" (Yamakawa et al., 1986), including all species with rows of hook-like denticles, (2) the "*Etmopterus pusillus*" group comprising *E. bigelowi* and *E. pusillus* displaying conical dermal denticles (Shirai and Tachikawa, 1993), and the (3) "*Etmopterus splendidus*" group, consisting of species, which show similarities in the shape of flank markings as well as arrangement of dermal denticles (Last et al., 2002). The monotypic etmopterid genera *Trigonognathus, Miroscyllium* and *Aculeola* each display genus-specific morphological features, such as highly protrudable jaws armed with characteristically shaped, single-cusped teeth without lateral cusplets (*Trigonognathus*), small and slender erect teeth in both jaws (*Aculeola*), or a combination of a "cutting–clutching type" dentition in subadults, and a "clutching type" dentition in adults (*Miroscyllium*). *Centroscyllium* includes seven described species with a dignathic homodont dentition, displaying morphologically highly similar teeth in both jaws. Further characters are differently shaped and sparsely spaced dermal denticles, and no conspicuous flank markings with the exception of *Centroscyllium ritteri*.

First efforts to understand the intrarelationships of Etmopteridae were carried out by Shirai and Nakaya (1990b) based on 15 osteological and myological characters of 14 species representing four genera. In this study, the authors defined the new genus *Miroscyllium* for *Centroscyllium sheikoi* based on morphological characters that combine both genera, *Etmopterus* and *Centroscyllium*. The sample size was increased to 19 described species in Shirai's Squalean phylogeny (1992) now also including the rare *Trigonognathus*. This latter study confirmed the monophyly of the four analyzed etmopterid genera within Squaliformes as previously suggested by Compagno (1973, 1984) and Cadenat and Blache (1981) and placed *Trigonognathus* as sister to *Aculeola* and *Centroscyllium*. Although being an important step forwards, further intragroup relationships especially with regard to the speciose genus *Etmopterus* could not be resolved and re-examinations of Shirai's dataset (1992) by Carvalho and de Maisey (1996) and Adnet and Cappetta (2001) led to different results (Adnet et al., 2006).

The large and continuously increasing species number within Etmopteridae, one of the most diverse families within Chondrichthyes, as well as a number of unresolved questions related to their biology and radiation provoked us to apply DNA based molecular phylogenetics to a new and extensive worldwide sampling of etmopterids to provide 20 years after Shirai and Nakaya's (1990b) initial study new insights into the taxonomy and evolution of these still poorly known family of bioluminescent deep-sea sharks. Specifically, we compiled an extensive DNA dataset to (1) identify the sister-group of Etmopteridae among Squaliformes, to (2) test for the monophyly of Etmopteridae and for the (3) independent development of bioluminescence within Squaliformes, to (4) test for the monophyly of each of the two polytypic etmopterid genera, to (5) test for a Lower Eocene origin of Etmopteridae as indicated by the fossil record, to (6) analyse sequential versus rapid speciation in the course of the speciose etmopterid radiation and (7) compare our molecular phylogeny with results based on morphological analyses.

2. Material and methods

2.1. Taxon sampling

Tissue samples were obtained from museum tissue collections or recently collected during deep-sea commercial fisheries or during fisheries monitoring programs and represent 26 of the extant 43 etmopterid species plus 13 samples being either unidentified or identification is preliminary. Species missing for a complete taxon sampling of extant Etmopteridae were too difficult to attain, since they are only known from very few specimens and remote locations (e.g. Springer and Burgess, 1985; Kotlyar, 1990). However, our sampling includes all five genera traditionally assigned to Etmopteridae and all previously identified species groups are well represented. In addition, representatives of the remaining five squaliform families Centrophoridae, Oxynotidae, Somniosidae, Dalatiidae, and Squalidae as well as Echinorhinidae were included in our analyses. *Odontaspis ferox* (Lamnidae), *Apristurus longicephalus* (Pentanchidae as defined in Iglésias et al., 2005) and *Chimaera* sp. (Chimaeridae) were chosen as chondrichthyan outgroups. For a list of all included species, specimen vouchers and Genbank Accession Numbers see Supplementary Material 1.

2.2. DNA-extraction, locus sampling, PCR and sequencing

Total genomic and mitochondrial DNA was extracted from muscle tissue or fin clips either preserved in 96% ethanol or 20% DMSO salty solution using the QIAmp tissue Kit (Qiagen®, Valencia, CA).

We targeted partial fragments of one nuclear gene and four mitochondrial loci, which provide sufficient phylogenetic signals for both ancient and more recent divergence in elasmobranchs (compare Iglésias et al., 2005; Maisey et al., 2004; Naylor et al., 2005; Ward et al., 2005; Ward et al., 2007): a portion of the nuclear RAG1 gene (1454 bp), portion of the mitochondrial gene Cytochrome Oxidase I (COI, 655 bp) which is established as potential "barcoding gene" for identifying species of sharks (e.g. Ward et al., 2005; Ward et al., 2007), partial tRNA-Phe, the full 12S rRNA and partial 16S rRNA including the Valine tRNA (2606 bp when aligned). All loci were amplified using PCR following the protocol of Iglésias et al. (2005). PCR products were cleaned using the

QIAquick PCR Purification Kit (Qiagen®, Valencia, CA) after the manufacturer's protocol. Cycle sequencing was performed using ABI Big Dye 3.1 chemistry (PE Applied Biosystems®, Foster City, CA). If necessary, internal sequencing primers were designed for attaining sequences from problematic samples. A summary of primers used in this study is given in Table 1.

2.3. Phylogenetic analyses

2.3.1. Alignment

Sequences were edited using the BioEdit software version 7.0.9 (Hall, 1999) and aligned with MUSCLE 3.6 (Edgar, 2004). Aliscore v.0.2 was used to check aligned single loci for ambiguous alignment positions (Misof and Misof, 2009). All loci were aligned separately and combined afterwards with BioEdit. For analysing homogeneity of base frequencies a X^2-test was performed with PAUP* v4b10 (Swofford, 2003). Phylogenetic analyses were conducted on the smallest resulting sequenced fragments homologous to all taxa which match an overall sequence size of 4685 bp per specimen. The first 1437 bp are portion of the RAG1 gene, following 2594 bp representing non-protein coding mtDNA fragments and the last 654 bp of the concatenated multigene alignment were attained from the coding mitochondrial COI gene. Confirmation of aligned single loci for coding RAG1 and COI was done by translating sequences into amino acids. Ambiguous sites in sequences, attributed to double peaks in the electropherogram were coded referring to IUB symbols. Transition and transversion rates (ts–tv) among third codon positions of coding gene regions were examined by comparing absolute distances in PAUP* (Swofford, 2003).

2.3.2. Maximum parsimony (MP)

MP analyses were carried out using PAUP* and the heuristic search option using the tree bisection reconnection branch swapping algorithm (tbr), which adds sequences of taxa randomly. A limit of 100 rearrangements was set, parsimony uninformative characters were excluded from the analyses, gaps were treated as missing data and characters were not weighted. We performed non-parametric bootstrapping with 1000 bootstrap replicates and 10 random additions.

2.3.3. Model selection using Bayes' factor test (BFT)

To test our dataset for suitable substitution models and corresponding partitioning avoiding over-parameterisation, a Bayes' Factor Test was conducted with MRBAYES (v3.1.2 Huelsenbeck and Ronquist, 2001; Nylander et al., 2004). Eight different partition strategies were tested for their best-fitting model or model combinations, respectively. Bayes' factors were computed calculating harmonic means with 100 bootstrap replicates. Analyses of likelihoods attained with MRBAYES were performed with Tracer v1.4

Table 1
Primers used for amplification and sequencing.

Primer	Sequence 5′–3′	Length (bp)	Forward/reverse	PCR	Sequencing	Site of fixation	Area
Chon-Mito-S003[a]	TCTCTGTGGCAAAAGAGTGG	20	F	X	X	1421–1440	Non-coding mtDNA
Chon-Mito-S005[a]	AGGCAAGTCGTAACATGGTAAG	22	F	X	X	0988–1009	Non-coding mtDNA
Chon-Mito-R008[a]	CCACTCTTTTGCCCACAGAGA	20	R		X	1421–1440	Non-coding mtDNA
Chon-Mito-S009[a]	CACGAGAGTTTAACTGTCTCT	21	F		X	2158–2178	Non-coding mtDNA
Chon-Mito-R010[a]	TAGAGACAGTTAAACTCTCGT	21	R		X	2159–2179	Non-coding mtDNA
Chon-Mito-S014[a]	AGTGGGCCTAAAAGCAGCCA	20	F		X	1665–1684	Non-coding mtDNA
Chon-Mito-R017[a]	ATCCAACATCGAGGTCGTAAACC	23	R		X	2526–2548	Non-coding mtDNA
Chon-Mito-S032[b]	AAG(CT)AT(AG)GCACTGAAGATGCTA	22	F	X	X	0020–0041	Non-coding mtDNA
Chon-Mito-S033[b]	ACTAGGATTAGATACCCTACTATG	24	F	X	X	0505–0528	Non-coding mtDNA
Chon-Mito-R034[b]	CGCCAAGTCCTTTGGGTTTTAAGC	24	R	X	X	0596–0619	Non-coding mtDNA
Chon-Mito-R035[b]	(CT)CCGGTCCTTTCGTACTAGG	20	R		X	2670–2689	Non-coding mtDNA
Chon-Mito-S037[b]	TGACCGTGC(AG)AAGGTAGCGTAATC	24	F		X	2098–2121	Non-coding mtDNA
Chon-Mito-R038[b]	TCTTC(CT)C(AC)CTCTTTTGC(AC)ACAGAG	24	R		X	1422–1445	Non-coding mtDNA
Chon-Mito-R039[b]	CAG(AG)TGGCTGCTT(CT)TAGGCC(CT)ACT	24	R		X	1665–1688	Non-coding mtDNA
Chon-Mito-R041[b]	(CT)CCGGTCCTTTCGTACT(AG)GG	20	R	X	X	2670–2698	Non-coding mtDNA
Chon-Mito-S043[b]	AGACGAGAAGACCCTATGGAGCTT	24	F		X	2233–2256	Non-coding mtDNA
Chon-Mito-R044[b]	AAGCTCCATAGGGTCTTCTCGTCT	24	R		X	2233–2256	Non-coding mtDNA
Fish F2 Barcode[c]	TCGACTAATCATAAAGATATCGGCAC	26	F	X	X	6448–6474	mtDNA, COI
Fish R2 Barcode[c]	ACTTCAGGGTGACCGAAGAATCAGAA	26	R	X	X	7152–7127	mtDNA, COI
S0156 Barcode[b]	TAGCTGATGAATCTGACCGTGAAAC	25	F	X	X	5458–5491	mtDNA, COI
R084 Barcode[b]	TGAACGCCAGATTTCATAGCGTTC	24	R	X	X	6177–6204	mtDNA, COI
Chon-Rag1-S018[a]	ACAGTCAAAGCTACTAC(AG)GGGA	22	F	X	X	2576–1597	nDNA, RAG1
Chon-Rag1-S019[a]	TGGCAGATGAATCTGACCATGA	22	F	X	X	2096–2117	nDNA, RAG1
Chon-Rag1-S020[a]	TGTGAACTGAT(CT)CCATCTGAAG	22	F		X	2719–2740	nDNA, RAG1
Chon-Rag1-R021[a]	AATATTTTGAAGTGTACAGCCA	22	R		X	3094–3115	nDNA, RAG1
Chon-Rag1-R022[a]	CTGAAACCCCTTTCACTCTATC	22	R		X	2440–2461	nDNA, RAG1
Chon-Rag1-R023[a]	CCCATTCCATCACAAGATTCTT	22	R		X	1904–1925	nDNA, RAG1
Chon-Rag1-S024[a]	CAGATCTTCCAGCCTTTGCATGC	23	F	X	X	1600–1622	nDNA, RAG1
Chon-Rag1-R025[a]	TGATG(CT)TTCAAAATG(CT)CTTCCAA	23	R		X	3070–3092	nDNA, RAG1
Chon-Rag1-S026[a]	TTCC(TA)GCCTTTGCA(CT)GCACTCCG	23	F	X	X	1606–1628	nDNA, RAG1
Chon-Rag1-S027[a]	GAGA(CT)TCTCAGAGAGTTAATGCA	23	F		X	2749–2771	nDNA, RAG1
Chon-Rag1-R028[a]	GT(CT)TCATGGTCAGATTCATC(CT)GC	23	R		X	2098–2120	nDNA, RAG1
Chon-Rag1-R029[a]	AGTGTACAGCCA(AG)TGATG(CT)TTCA	23	R	X	X	3083–3105	nDNA, RAG1
Chon-Rag1-S030[a]	GTGAG(AG)TATTCCTT(CT)AC(AC)ATCATG	24	F		X	1975–1998	nDNA, RAG1
Chon-Rag1-S031[a]	GA(AG)CGCTATGAAAT(CT)TGGCGTTCA	24	F		X	2383–2406	nDNA, RAG1
Chon-RAG1-S-trigo[d]	GTGTAAGTGTGATGAATGA	19	F		X	1666–1684	nDNA, RAG1
Chon-RAG1-R-trigo[d]	ACATAGCGTTCCAAGTTCTC	20	R		X	2374–2393	nDNA, RAG1
Chon_RAG1-R019[d]	TCATGGTCAGATTCATCTGCCA	22	R	X	X	2096–2117	nDNA, RAG1

[a] Primers from Iglésias et al. (2005).
[b] The position of the primers refers to the 5′–3′ position in the complete mitochondrial genome sequence of *Amblyraja radiata* (GenBank Accession No. NC_000893.1).
[c] Primers from Ward et al. (2005).
[d] Internal PCR and sequencing primers designed for this study.

(http://beast.bio.ed.ac.uk). Bayes' factors favoured a partition of the data for ML and Bayesian phylogenetic analyses into (1) a single partition for RAG1, (2) a single partition for the large ribosomal mitochondrial fragment encompassing tRNA-Phe, 12S rRNA, 16S rRNA and the valine tRNA, and (3) two further partitions for COI, one for a combined 1st and 2nd position and one for the third codon position. For RAG1 and 3rd codon position of COI, the HKY Gamma substitution model revealed highest likelihood scores, whereas for the large ribosomal fragment and COI 1st and 2nd positions the GTR Gamma model was favoured.

2.3.4. Maximum likelihood (ML)

ML analyses were performed using RaxML ver. 7.0.3 (Stamatakis, 2006). A hill-climbing algorithm is used for analyses using the GTR Gamma nucleotide substitution model. Several runs were conducted to avoid local maxima in the space of trees. The partition scheme follows results attained from the Bayes' Factor test (see Section 2.3.3). Initially, runs were carried out using the RaxML option of automatically generated MP starting trees. Maximum likelihoods of fixed initial rearrangement settings were compared with likelihoods obtained from automatically generated settings. Rate category number was set to 25 after testing values of 10–55 in steps of five rate categories as recommended in the RaxML manual. For attaining support values for nodes in the ML tree, bootstrapping was performed with 150 bootstrap replicates after assessment of a reasonable number of bootstrap replicates (Pattengale et al., 2009) using the option to search for an adequate number of bootstrap replicates implemented in RaxML v7.1.0. Branches showing bootstrap support below 50% were collapsed. Analyses were performed for single loci, nuclear versus mitochondrial, and combined datasets.

2.3.5. Bayesian phylogenetic analyses

MRBAYES v3.1.2 software was used for Bayesian phylogenetic reconstruction under a partitioning scheme as described under Section 2.3.3. Two independent analyses were performed under the option of random starting trees and four simultaneous Markov Chains (three heated and one cold chain). Trees were sampled every 1000 generations in an overall run of 10.000.000 generations. After checking the likelihood values with the plot option of MRBAYES, the first 25% of generations were discarded as burn-in and a 50% majority rule consensus tree was computed from trees showing likelihoods of stationarity. Again, analyses were performed for single loci, nuclear versus mitochondrial and concatenated datasets.

2.3.6. Node age reconstruction based on fossil calibration points

Several problems appear when searching for suitable fossils as calibration points for implementing a meaningful molecular clock approach in an etmopterid phylogeny. On the one hand fossil remains of etmopterids comprise fossilized teeth only and few studies exist dealing with the identification of general morphological tooth characteristics for identifying genera (Adnet and Cappetta, 2001; Kriwet and Klug, 2010; Straube et al., 2008). On the other side, dating of geological strata including fossil remains of Etmopteridae are partially debatable (Adnet et al., 2006). Therefore we used only a set of five comparatively undebatable fossil calibration points. The five calibration points are stated in the following as mean ages of stratigraphic ranges and represent minimum ages. Our first point provides a minimum age for the root of the tree using the first unambiguous chimaeroid fossil dated to 374.5 Ma in the late Devonian (Venkatesh et al., 2007; Benton and Donoghue, 2007). Further, we restricted the minimum age of Squaliformes to a time window of 130–125 Ma ago in the early Cretaceous, as indicated by fossil findings of teeth of Protosqualus (Cappetta, 1987), apparently the oldest known representative of

Squaliformes suggested by its tooth root morphology (Kriwet and Klug, 2010) and assuming that Protospinax is not a squaliform shark (Kriwet and Klug, 2004). Further calibration points within Squaliformes comprise the minimum age of Centroscymnus ranging from 83.5 to 70.6 Ma (Thies and Müller, 1993) and Centrophoridae with 70.6 to 65.5 Ma referring to articulated fossils from Sahel Alma, Lebanon (Cappetta, 1987) displaying the desired clear linkage to extant species. Finally, the age of Trigonognathus/Etmopterus was set to a mean minimum age of 44.5 Ma in the Eocene as indicated by fossil teeth of Trigonognathus virginiae, which are morphologically highly similar to teeth of the extant Trigonognathus kabeyai (Cappetta and Adnet, 2001).

Node age reconstruction was performed in using the penalized likelihood approach implemented in r8s (Sanderson, 2002; Sanderson, 2003) as well as the Bayesian approach implemented in BEAST (v.1.4.7 Drummond and Rambaut, 2007). In both cases, all five calibration points and the Bayesian majority consensus tree topology in the Newick format were used as starting points for calculating chronograms.

For estimating unknown node ages in r8s, non-parametric rate smoothing was conducted via cross-validation and resulted in a smoothing parameter of 1.6e + 02. Our five calibration points were assumed as constrained node ages, allowing r8s to estimate divergence times. Minimal and maximal age constraints were set to cover stratigraphic ranges of fossil findings (Table 2). A bootstrapping procedure was conducted with the help of the r8s-bootstrap Kit (Eriksson, 2007) to attain confidence intervals on parameters. Here, we reproduced 100 pseudo replicates from the original alignment with Seqboot implemented in Phylip v3.6.7 (Felsenstein, 2005). For each replicate, a cross-validation analysis was performed to find optimal smoothing parameters. Thereafter, confidence intervals were calculated.

For estimating node ages with Bayesian inferences, the BEAST programme package (Drummond and Rambaut, 2007) was used. We created XML files with BEAUti containing a starting tree and calibration points. Node ages of calibration points were implemented assuming different prior distributions. The analyses assumed a relaxed molecular clock approach under the assumption of an uncorrelated lognormal model (UCLN Drummond et al., 2006) and the substitution models and data partitioning following the results of the BFT (see Section 2.3.3). The Yule speciation process was chosen as tree prior, assuming a constant speciation rate per lineage (Drummond and Rambaut, 2007), and a Markov Chain lasting 30 million generations. Tracer v.1.4 was used for checking performed runs for reaching stationarity regarding the posterior probabilities and confirming adequate effective sample sizes (ESS) in final runs. A burn-in of 25% of all sampled trees was discarded. Log-Combiner was employed to combine trees and log files attained from several identical runs, which were combined afterwards to decrease computational times. TreeAnnotator allowed to create consensus trees and FigTree v.1.1.2 enabled the visualization of the attained chronograms. We used three strategies to attain reliable node age estimates. First, we performed a run assuming a normal distribution as prior settings for calibration points. Means and standard deviations of calibration point ages were chosen to cover the range of stratigraphic stage ages where fossils used as calibration points were discovered. This run was conducted to roughly pre-date the tree for further runs with a Markov Chain lasting one million generations only. In a second step, the resulting chronogram from our first run was implemented as starting tree for a re-run with BEAST since the node ages from our pre-dating run fell into the time ranges of our calibration points. This time, the fossil calibration points were used under the assumption of an exponential prior, explaining the data more efficiently, because absolute dates can hardly be given in terms of calibration with fossils in contrast to an exponential prior

Table 2
Fossil calibration points used for node age estimation.

Calibration point	Age (mya)	Stage	References
Chimaeriformes	374.5–359.2	Upper Devonian, Fammenian	Benton and Donoghue (2007), Venkatesh et al. (2007)
Squaliformes	130.0–125.0	Lower Cretaceous, Barremian	Cappetta (1987)
Somniosidae	83.5–70.6	Upper Cretaceous, Campanian	Thies and Müller (1993)
Centrophoridae	70.6–65.5	Upper Cretaceous, Maastrichtian	Cappetta (1987)
Splitting *Trigonognathus/Etmopterus*	44.5–40.4	Palaeogen, Middle to Upper Lutetian	Cappetta and Adnet (2001)

assuming the genus to be present some time before the occurrence of the fossil which most probably does not represent the first occurrence. Zero-offsets adopted node ages reconstructed from the pre-dating analyses using normally distributed prior settings and exponential means were chosen, as in our first run, to cover the age of stratigraphic ranges of fossil findings of used calibration points. Here, two identical runs were performed lasting 30 million generations each, which subsequently were combined.

In a third step, we implemented the attained r8s chronogram as starting tree in BEAST following Hardman and Hardman (2008) for reassessing results from both, ML and Bayesian node age reconstructions. This step was conducted to obtain an independent measure for the accuracy of our node age estimation. The run lasted 30 million generations.

Finally, the same procedure was conducted again, only differing in calibration points to get a measure for the influence of calibration points on node age reconstructions. In additional runs operated in BEAST, we eliminated either the node age calibration of Centrophoridae or Somniosidae to obtain insights into the variability of results. Performed runs which were not calibrated with fossils displayed older node ages and larger confidence intervals as expected. See Table 2 for fossil calibration points used in this study.

3. Results

3.1. Sequence characteristics and phylogenetic signal

The sequenced portion of the RAG1 gene shows 925 constant characters, of which 265 are parsimony non-informative and 247 parsimony informative. As expected, RAG1 displays a smaller number of parsimony informative characters compared to the mtDNA dataset (constant characters = 1933, variable parsimony non-informative = 422 and parsimony informative = 1007). The X^2-test revealed equally distributed base frequencies for all loci (df = 216, all $p > 0.9$). For empirical base frequencies of single loci see Table 3. Translation of coding genes RAG1 and COI into amino acids showed no stop codons or improbable frame shifts. Inspection of transition–transversion rates (ts–tv) showed no saturation for third codon positions of coding genes.

3.2. Phylogenetic analyses

ML, Bayesian and MP analyses yielded almost identical phylogenetic hypotheses with regard to the well supported monophyly of Squaliformes and Etmopteridae as well as for major etmopterid intrarelationships, but failed to unambiguously identify the sistergroup of Etmopteridae. Fig. 1 provides an overview of obtained tree topologies as a BI dendrogram with statistical support values for

Table 3
Empirical base frequencies.

| Area	Pi (A)	Pi (G)	Pi (T)	Pi (C)
RAG1	0.323437	0.243525	0.256767	0.176271
CM	0.346216	0.176951	0.270659	0.206174
COI	0.259488	0.168938	0.332910	0.238664

ML and BI. Supplementary Materials 2 and 3 supply BI and MP phylograms with bootstrap or posterior probability values.

Within Squaliformes only the basal split of *Squalus* (Squalidae) from the rest of Squaliformes is strongly supported, whereas most relationships within other families of Squaliformes were not supported with high support values. However, all analyses render Somniosidae sensu Compagno et al. (2005) to be paraphyletic with respect to Oxynotidae (represented here by *Oxynotus paradoxus*). In addition, separate analyses of the RAG1 dataset including *Echinorhinus brucus* (Echinorhinidae) and *Isistius brasiliensis* (Dalatiidae) strongly suggest that these are not the sister-clades of Etmoperidae, although the full sequence dataset including mitochondrial loci could not be amplified for these taxa (Fig. 3).

Intrafamilial relationships of Etmopteridae identify nine major clades, each supported with 99–100% bootstrap support in ML and MP analyses or 1.00 posterior probabilities in BI (Fig. 1). Interrelationships of these clades are not always well supported. In combined mtDNA and RAG1 analyses, *Trigonognathus kabeyai* (clade I) is sister to *Etmopterus*, whereas employing RAG1 alone identifies *Trigonognathus* as sister to the *Aculeola/Centroscyllium* clade (clades VIII and IX, Fig. 1). *Aculeola* (clade IX, Fig. 1), a monotypic genus endemic to the southeastern Pacific, is identified with strong support as the sistergroup of *Centroscyllium* (clade VIII, Fig. 1), a genus comprising seven species, four of which could be sampled in our dataset. *Centroscyllium* mainly occurs in temperate southern ocean basins. The rarely caught *Miroscyllium sheikoi*, another monotypic genus known from southern Japan and Taiwan only, occurs in all analyses within the *Etmopterus lucifer* clade (clades IV, V and VI, Fig. 1), and thus renders *Etmopterus* paraphyletic.

Etmopterid intrageneric phylogenetic analyses of the speciose genera *Etmopterus* and *Centroscyllium* partially revealed multiple and previously undetected hypotheses with high support values in all analyses. *Etmopterus* is not monophyletic with regard to *Miroscyllium* (see above) and is split into two major sister clades. The first monophylum comprises two clades, the mostly panoceanic temperate *E. spinax* clade, previously unrecognised (clade II, Fig. 1) and named after the type species of the genus *Etmopterus* Rafinesque 1810, and the (sub-) tropical Atlantic *E. gracilispinis* clade, previously unrecognised (clade III, Fig. 1). The second major monophylum comprises four clades, including *Miroscyllium sheikoi* (clade IV, Fig. 1), the paraphyletic traditional *Etmopterus lucifer* group, split into clades V and VI (Fig. 1) and the panoceanic *E. pusillus* clade (clade VII, Fig. 1). The *E. lucifer* clade (clades IV, V, and VI, Fig. 1) represents a monophylum which is sister to clade VII. Interestingly, *Miroscyllium* is sistergroup to clade V, part of the *E. lucifer* clade comprising specimens from the northern hemisphere only. Most terminal taxon-relationships at species level were resolved with high statistical support. However, we detected multiple occurrences of species level paraphyly indicating either misidentifications or previously undetected cryptic diversities, e.g. within the *E. spinax* clade (*Etmopterus unicolor, Etmopterus* sp. B, *Etmopterus* cf. *granulosus*). For phylogenetic placement and geographic origin of terminal taxa, see Fig. 1 and Supplementary Material 1.

The second comparatively species rich etmopterid genus *Centroscyllium* is represented by four species in our analyses (out of seven described): *C. fabricii* (Northern Atlantic) and *C. ritteri* (Japan)
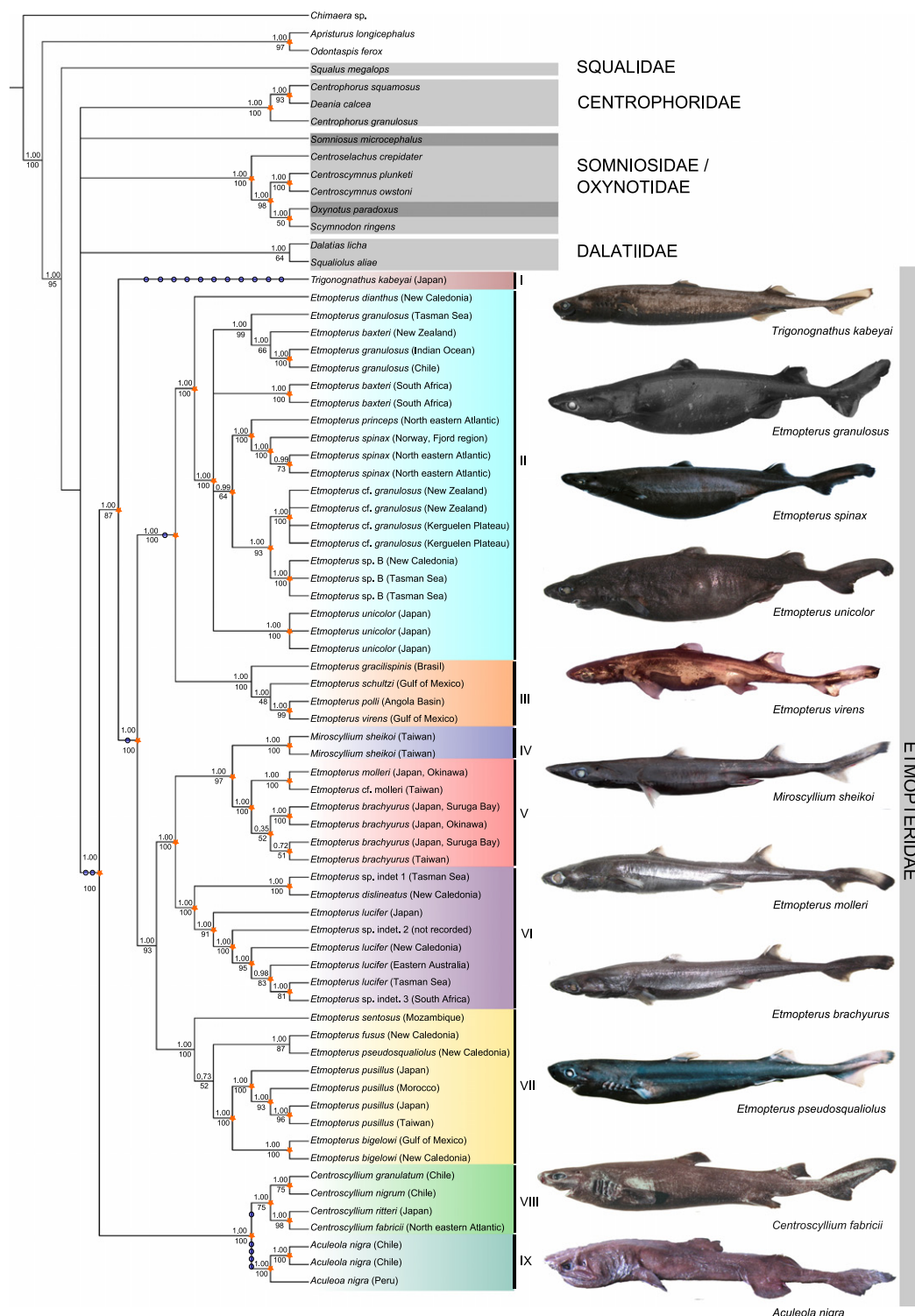
Fig. 1. Dendrogram displaying phylogenetic relationships of Etmopteridae, reconstructed with Bayesian inference. Widely congruent topologies were attained with ML and MP analyses. Numbers above internal nodes indicate posterior probabilities (PPs) from Bayesian analyses, numbers below branches bootstrap scores attained from ML search strategies. Orange asterisks refer to nodes found in MP analysis with a bootstrap support >50%. Nodes displaying PPs and bootstrap scores <0.95 (PP) and <50% (bootstrap support) were collapsed. Blue circles refer to synapomorphic morphological character states found by Shirai (1992) which are in congruence with our tree topology (see Table 5). Roman numerals refer to nine major clades resulting from phylogenetic analyses. Among the speciose genus *Etmopterus*, four clades can be identified, partially morphologically characterizable: *E. spinax* clade (clade II), *E. gracilispinis* clade (clade III), *E. lucifer* clade (clades IV, V and VI), and *E. pusillus* clade (clade VII): Etmopterus sp. indet. 1: preliminary identified as *Etmopterus* cf. *molleri*; *Etmopterus* sp. indet. 2: preliminary identified as *E. lucifer*; *Etmopterus* sp. indet. 3: preliminary identified as *Etmopterus* cf. *brachyurus*. Dark grey colours mark taxa differing from traditional squaliform families (light gray).

forming a subclade opposite to the South American endemics *C. nigrum* and *C. granulatum*. The monophyly of the genus is significantly supported (Fig. 1).

Seventeen of 27 morphological synapomorphies described by Shirai (1992) are in concordance with our molecular tree topology (Fig. 1, Table 5).

3.3. Node age reconstruction

Our partitioned Bayesian estimates of node ages using the BEAST program package were largely congruent with results attained using the penalized likelihood approach as implemented in r8s (Fig. 2 and Table 4). We based our analysis on the Bayesian tree (see Supplementary Material 2), but refer here only to well supported nodes as shown in Fig. 1. With regard to outgroups of Squaliformes, the early split of monophyletic Squaliformes from Lamniform and Carcharhiniform lineages (*Odontaspis* and *Apristurus*, respectively), occurred some 170 (218–133) Ma ago, and the split between *Apristurus* from *Odontaspis* is stated to 84 (134–30) Ma, but confidence intervals for these nodes are large. In contrast, the age of Squaliformes is estimated comparatively precisely around 128 (130–127) Ma, and the age of origin of the squaliform families Centrophoridae is 71 (74–69 Ma), Dalatiidae 67 (68–67 Ma) and Somniosidae 69 (70–67 Ma; excluding *Somniosus*). Although sister-family relationships among Squaliformes could not be satisfactorily resolved and resulted in a polytomy (Fig. 1), the different families form monophyla, whose minimum ages can be estimated using fossil calibration points, i.e. Centrophoridae and Somniosidae. *Somniosus* is not included in Somniosidae sensu Compagno et al. (2005) but support values are weak. Therefore the branch was collapsed and treated as a separate monophyletic group neighbouring remaining squaliform families. Intrafamilial diversification of the respective families stated at 45 (64–26) Ma for Dalatiidae, 40 (61–19) Ma for Centrophoridae and Somniosidae (without *Somniosus*) are dated to 37 (53–20) Ma. Confidence intervals are large but broadly overlapping.

The age of our focus group Etmopteridae is dated as the splitting between *Somniosus* and etmopterids and must have occurred at the end of the Cretaceous or beginning of the Paleocene, about 61 (69–53) Ma ago. We highlight here, that the sister-group relationship between *Somniosus* and Etmopteridae as depicted on the basis of the Bayesian phylogenetic hypothesis (Fig. 1, Supplementary Material 2), is only weekly supported and therefore the precise age of origin remains questionable. With Etmoperidae, the major divergence of the *Aculeola*/*Centroscyllium* clade from the remaining clades is estimated to be ca. 44 (48–41) Ma ago, and further divergence of *Aculeola* from *Centroscyllium* to 23 (39–12) Ma ago. Taxon sampling of *Centroscyllium* is incomplete preventing an age estimate for the genus. However, *Aculeola* with only one known species to date seems to be comparatively old with a split age of 11 (18–4) Ma ago for the Peruvian and Chilean samples. The age of the next split within Etmopteridae is the divergence between *Trigonognathus* and the *Etmopterus*/*Miroscyllium* – lineage, which is dated to 41 (46–36) Ma based on the calibration point using the *T. virginiae* fossils. The early steps of the *Etmopterus*/*Miroscyllium* radiation into multiple subgroups (clade II-*E. spinax* clade, III-*E. gracilispinis* clade, IV, V and VI-*E. lucifer* clade, and VII-*E. pusillus* clade) apparently took place in a comparatively narrow time window between 31 and 40 Ma. As the taxon sampling for the *Etmopterus* radiation is fairly complete, we assume that time estimates for subgroup origins are close to real group diversification ages, but age estimates are nevertheless overlapping. The divergence of the two major etmopterid clades (clades II + III sister to clades IV, V, VI, and VII) containing two subclades each date to 36 (42–32) Ma. The *E. spinax* clade (clade II) separates from the *E. gracilispinis* clade (clade III) around 30 (36–22) Ma ago, a similar age as compared to the *E. lucifer* clade (clades IV, V, and VI) and *E. pusillus* clade (clade VII, ca. 33 (39–27) Ma). The youngest subgroup is apparently the *E. spinax* clade (clade II), which radiated some 14 (21–8) Ma ago. The *E. gracilispinis* clade (clade III) shows an older radiation age, which is dated to 22 (29–14) Ma. clades IV, V, VI and VII on average evolved 33 (39–27) Ma ago, displaying radiation dates for the *E. lucifer* clade 24 (32–17) Ma ago, but for *Miroscyllium* of only 19 (27–11) Ma. Radiation events of clades V and VI (the Northern and Southern Hemisphere species of the *E. lucifer* clade)
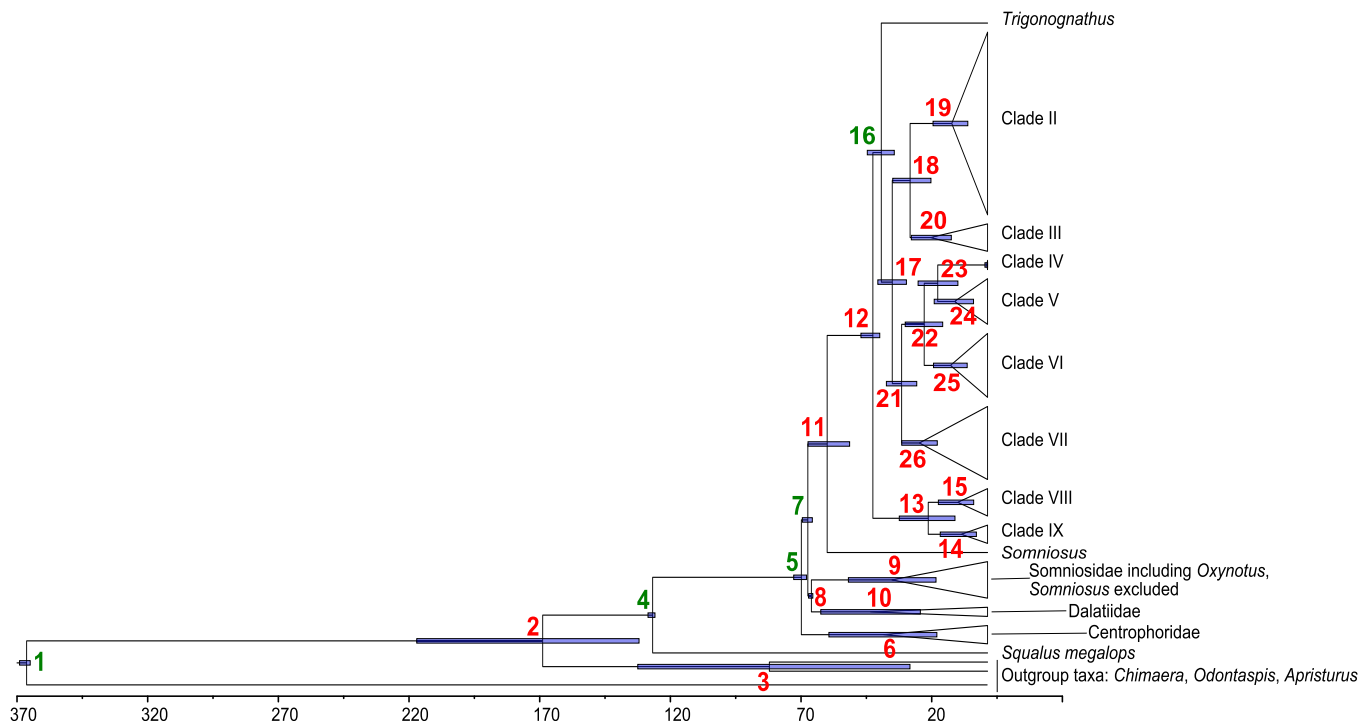

Fig. 2. Estimated divergence times attained from Bayesian and Penalized Likelihood methods. Red numbers refer to node numbers given in Table 4 including node descriptions, mean node ages and confidence intervals of both analysing approaches. Green numbers indicate applied calibration points attained from fossils. Origin of Etmopteridae in between 69 and 53 Ma, origin of genus *Etmopterus* in between 48 and 36 Ma with further radiation events from 14 to 36 Ma. (For interpretation of references to color in this figure legend, the reader is referred to see the web version of this article.)
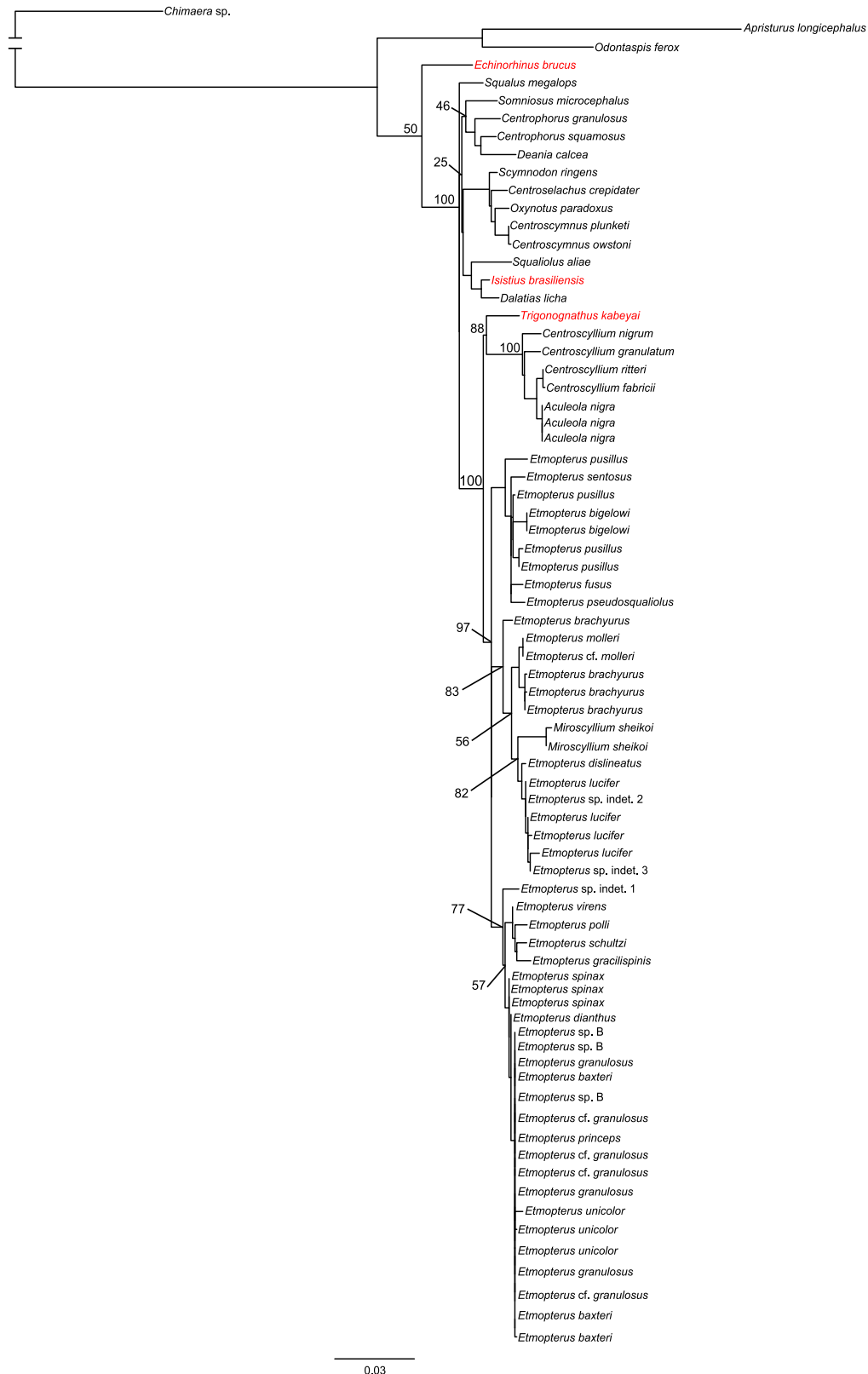
Fig. 3. Maximum likelihood based phylogram of RAG1 data, additionally including *Echinorhinus brucus* and *Isistius brasiliensis*. Red-coloured species represent additional taxa not included in the concatenated dataset and *Trigonognathus* controversial placement in analyses using RAG1 data only. (For interpretation of references to color in this figure legend, the reader is referred to see the web version of this article.)

also occurred comparatively recently with age estimates of 13 (20–5) and 14 (21–8) Ma, respectively. In contrast, the oldest clade, the *Etmopterus pusillus* clade (clade VII), started separation and diversi-

fication already 26 (33–19) Ma ago. The inferred confidence intervals were partially in concordance with ages calculated with the Bayesian tree as starting tree in r8s, but some confidence intervals

Table 4
Mean node ages and confidence intervals attained with different analysing approaches.

Node #	Node description	Age estimates BEAST		Age estimates r8s	
		Node age	Height 95% HPD	Node age	Height 95% HPD
1	Root age	367.70	366.33–370.4	369.51	366.33–370.52
2	Split Squaliformes	170.23	133.37–218.42	337.10	134.77–229.87
3	Split *Odontaspis* & *Apristurus*	83.51	29.70–133.85	241.72	40.64–144.29
4	Split *Squalus*	128.15	127.27–129.94	129.14	127.27–129.76
5	Split Centrophoridae	71.26	69.28–74.18	70.6	69.28–74.35
6	Radiation Centrophoridae	39.75	19.41–60.72	43.08	19.42–58.31
7	Split Etmopteridae & *Somniosus* from Somniosidae & Dalatiidae	68.78	67.06–70.89	–	67.04–70.99
8	Split Somniosidae/Dalatiidae	67.42	66.87–68.49	70.6	66.87–68.48
9	Radiation Somniosidae	36.64	19.73–53.26	37.83	20.80–54.211
10	Radiation Dalatiidae	44.83	25.73–63.83	62.34	21.59–64.84
11	Split *Somniosus*/ Etmopteridae	61.38	52.79–68.71	59.85	53.57–68.72
12	Split clades VIII & IX from clades I and II-VII	43.89	41.26–48.46	56.81	41.26–48.94
13	Split clades VIII & IX	22.70	12.48–38.78	40.78	15.47–39.90
14	Radiation clade IX	10.60	4.29–18.11	25.67	4.93–18.05
15	Radiation clade VIII	11.43	5.32–18.81	21.85	5.08–20.42
16	Split clades I & II–VII	40.67	35.70–46.02	44.25	36.26–47.70
17	Split up of clades II & III from IV, V & VI	36.48	31.55–41.36	34.24	31.67–42.76
18	Split clades II & III	29.65	21.67–36.29	30.34	22.88–37.17
19	Radiation clade II	13.71	7.57–20.87	23.59	7.64–20.12
20	Radiation clade III	21.80	13.88–29.17	29.54	14.02–29.68
21	Split clades IV, V & VI from VII	32.88	27.10–38.72	32.00	27.77–39.11
22	Splitting up of clades IV, V and VI	24.26	17.18–31.52	19.08	18.21–31.43
23	Split IV	19.06	11.36–26.59	15.02	11.72–26.88
24	Radiation clade V	12.63	5.38–20.42	7.73	5.89–19.91
25	Radiation *E. lucifer*, split *E. dislineatus* & *E.* sp. indet. 1	14.19	7.80–20.68	16.80	7.94–21.53
26	Radiation clade VII	26.07	19.24–32.85	18.69	19.32–33.97

displayed biases revealing unreasonable large confidence intervals, which can be explained by low likelihood scores of ML trees attained from the bootstrapped alignment. Using the chronogram attained with the Penalized Likelihood method in r8s as starting tree in BEAST aligns with results attained from the Bayesian tree as starting setting. A summary of node age estimations is provided in Fig. 2 and Table 4.

4. Discussion and conclusions

Phylogenetic reconstruction of extant Lantern Sharks (Etmopteridae), has been restricted to two studies primarily based on 27 osteological and myological characters up to now (Shirai, 1992; Shirai and Nakaya, 1990b). Additionally, several studies on elasmobranch interrelationships incorporated a single or few Lantern Shark species providing information about the sister-clade of Etmopteridae among Squaliformes (Compagno, 1973; Compagno, 1977; Maisey et al., 2004; Shirai, 1992). Our study is based both on more etmopterid taxa and significantly more characters and provide evidence for monophyly of Etmopteridae which comprise four major intrafamilial lineages (clades I–IX) corresponding largely but not fully to the four morphologically well diagnosable genera *Aculeola, Centroscyllium, Trigonognathus* and the highly diverse genus *Etmopterus* (Fig. 1).

4.1. Age and origin of Lantern Sharks

Our age estimate for the origin of Etmopteridae, which corresponds to the (not strongly supported) divergence between Etmopteridae and *Somniosus* (Figs. 2 and 3, Supplementary Material 2), agrees with the end of the Cretaceous and beginning of the Paleocene (Cretaceous/Tertiary boundary), respectively, and dates back substantially earlier than the first unambiguous etmopterid fossils from deep-water Eocene sediments (*Etmopterus bonapartei, E. acuticens, E. cahuzaci, Trigonognathus virginiae, Miroscyllium*, and *Paraetmoperus* (Adnet, 2006; Adnet et al., 2008; Cappetta and Adnet,

2001; Cigala, 1986; Ledoux, 1972)). According to our node age estimates as well as to the fossil record, all other squaliform deep-water inhabitants, i.e. Somniosidae, Centrophoridae, and Dalatiidae also originate around or shortly before the C/T boundary. Only the predominantly shallow water Squalidae, the sister-group to all deep-water squaliform sharks, as well as all ambiguously identified and now extinct "etmopterid" lineages from shallow waters (*Eoetmopterus, Microetmopterus* and *Proetmopterus*) are known from substantially before the C/T boundary (Adnet et al., 2006; Kriwet and Benton, 2004; Siverson, 1993; Cappetta and Siverson, 2001; Underwood and Mitchell, 1999). This pattern indicates that the major biotic crisis at the C/T boundary affected squaliform sharks in different ways. However, this interpretation has to be treated with caution, because the ML based age estimate for the *Somniosus*/Etmopteridae split displays large error bars and because a sister-clade relationship of Etmopteridae and *Somniosus* is not supported with high confidence in all our analyses. Further, it remains to be substantiated, that squaliform teeth fossils from the Turonian (93.5–89.3 Ma) are indeed a *Centrophorus* (Cappetta, 1987), which would invalidate our C/T boundary deep-water colonization hypothesis.

The four major etmopterid lineages differ mostly in specific dental characters indicating that trophic specialization played an important role for the early radiation of the group. According to our molecular clock estimates, this trophic radiation took place in the late Palaeocene/early Eocene between 48 and 41 Ma ago (Table 4). Subsequent evolution leading to the extant diversity of etmopterid genera occurred in the Middle Eocene to Early Miocene, approximately 45–15 Ma ago. Taking into account that this period (Palaeogene) is considered to represent the recovery phase after the extinction crisis at the C/T boundary (Kriwet and Benton, 2004; Stanley, 2009), the evolution of specialized dentitions in etmopterids may be the result of increased ecological opportunity after C/T extinction events as well as of the evolution of increased prey diversity in the post C/T boundary recovery phase, which e.g. led to a diversification of cephalopods (Lindberg and Pyenson, 2007), which form a major part of extant etmopterid diet (Klimpel et al., 2003; Neiva et al., 2006).

Table 5
Preliminary classification of Etmopteridae based on results of this study. *E. villosus* is not shown due to missing informations and samples for the present study. Morphological characteristics list synapomorphies diagnosed by Shirai (1992), which are in concordance with our molecular tree topology and general flank mark shapes of *Etmopterus* clades found in this study.

Genus	Clade	Morphological characteristics	
Aculeola		– secundary loss of fossa for rectus externus – double-pointed expansion of basihyal – double-pointed expansion of puboisschiadic bar – loss of the primary calcification of the centrum with a cylindrical notochordal sheath interrupted by a transverse septum	
Centroscyllium		– subnasal stay present	
Trigonognathus		– profundus canal present – suborbital keel-process lost secondarily – basibranchial copula very reduced (*Trigonognathus*-lype) – anterior basi-branchial absent – suborbitalis absent; constructor dorsalis arising from a seam of connective tissue at the middorsal line – posterior part of the intermandibularis inserting on ceratohyal – posterior slip of arcualis dorsalis lost secundarily – subspinalis externus present – pectoral propterygium fused with mesopterygium	
Etmopterus		– short eye-stalk, not reaching eye-ball	
	E. spinax & E. gracilispinis clades	– adductor mandibularis ß present	
	E. spinax clade (**clade II, Fig. 1**) *E. baxteri, E. dianthus, E. granulosus,* *E. litvinovi*. E. princeps. E. hillianus*,* *E. spinax. E. unicolor. E. sp. B*	– flank mark shape (if present) displaying long thin linear, anterior branches, and no or only weak posterior branches	
	E. gracilispinis clade (**clade III, 1, Fig. 1**) *E. gracilispinis, E. perryi*, E. polli,* *E. robinsi*, E. schultzi, E. virens*	– flank mark shape displaying long, thick, and curved anterior branches and short to medium thick posterior branches	
	E. lucifer clade (**clades IV, V, VI Fig. 1**) *E. brachyurus, E. burgessi*. E. bullisi*,* *E. decacuspidatus, E. dislineatus,* *E. evansi*, E. lucifer, E. molleri,* *E. pycnolepis* (excluding E. sheikoi)*	– flank mark shapes displaying long thin anterior branches and long thin, linear posterior branches exceeding anterior branch lengths	
	E. pusillus clade (**clade VII, Fig. 1**) *E. bigelowi, E. carteri*, E. caudistigmus*,* *E. fusus, E. pseudosqualiolus, E. pusillus,* *E. sentosus, E. splendidus**	– flank mark shapes displaying short, thick anterior branches and no or only weak posterior branches	
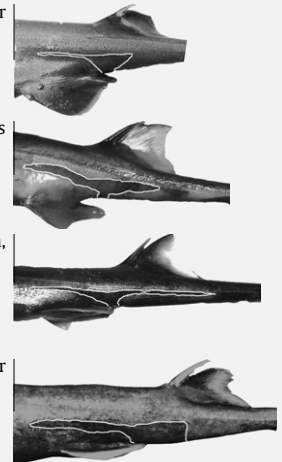
*Species not included in molecular analyses.

According to our analyses, intrageneric diversification within *Etmopterus* commenced at the Oligocene/Miocene boundary and continued well into the middle Miocene. It is interesting in this context, that a climatic shift from Palaeogene greenhouse conditions to icehouse conditions at the Eocene/Oligocene transition resulted in expanding Antarctic ice shields, the establishment of the circum-Antarctic current and subsequent chilling of the deep-sea (Eldrett et al., 2009; Lear et al., 2008). This coherence might indicate that the *Etmopterus* radiation was correlated with this significant climate change that established cooler temperatures which prevail until today. The cooling event allowed for the formation of eutrophic conditions at the seafloor, as known for example from palaeo-ecological studies from the western Tethys (Alegret et al., 2008). Cooling in coherence with steep continental slopes favours fast downslope transfer of organic material and consequently a rich benthic fauna especially of this part of the bathyal zone (Türkay, 2002). This establishment of nutritious food webs on the slopes is a prerequisite for rich feeding grounds for species ranking higher in food webs such as etmopterid sharks, or beaked whales (Cetacea: Ziphiidae). Interestingly, beaked whales with a similar depth penetration spectrum as Etmopteridae radiated roughly at the Oligocene/Miocene boundary, too (Dalebout et al., 2008).

4.2. Bioluminescence and the Etmopterus radiation

Our phylogenetic analyses of portions of the RAG1 gene place the bioluminescent dalatiid *Isistius brasiliensis* within a monophyletic group alongside with bioluminescent species *Dalatias licha* and *Squaliolus aliae* (Fig. 3). Although the sister-family relationships of Etmopteridae could not be clarified in our study, these results show that a monophyletic clade Dalatiidae evolved independently from Etmopteridae supporting the hypothesis that bioluminescence has evolved twice independently as suggested previously by several authors (Claes and Mallefet, 2008; Hubbs et al., 1967; Reif, 1985).

The reasons for the rapid and massive diversification of *Etmopterus* generating the most speciose clade of Squaliformes and one of the largest groups within Neoselachii may be discussed controversially. Trophic diversification based on alternatively adapted dentitions might be one reason. However, although the specific clutching–crushing type dentition of *Etmopterus* is unique among Etmopteridae the limited phenotypic diversity of tooth shapes within the genus cannot explain the evolution of more than 30 species. In addition, this type of dignathic heterodonty (cuspid teeth in the upper jaw, blade-like, overlapping teeth in the lower jaw) evolved in Centrophoridae, Dalatiidae and Somniosidae, too, but

without producing increased species richness. In contrast, the ability to emit light via photophores (bioluminescence) is limited among sharks to Dalatiidae and Etmopteridae. Here, bioluminescence may serve several functions: first, ventrally located photophores may provide counter illumination to serve as camouflage against residual sunlight when viewed from below (Claes and Mallefet, 2008; Reif, 1985; Widder, 1998).

Second, species specific bioluminescent flank markings may be interpreted as visual cues enabling species recognition, and, in combination with social interactions as schooling. Those flank markings are not present in bioluminescent Dalatiidae, *Aculeola*, and most *Centroscyllium* species, but they are highly diverse within *Etmopterus*. In *Etmopterus* it has even been hypothesized to aid cooperative hunting in closely interacting conspecific packs (Claes and Mallefet, 2008, 2009; Reif, 1985). The latter behaviour is assumed both for *E. virens* (Springer, 1967) and for *E. spinax* (Macpherson, 1980). Stomach food content analyses of *E. spinax* revealed very large prey chunks, but may be explained by scavenging behaviour instead of cooperative hunting of large prey (Neiva et al., 2006). In the case of sympatry, markings may enhance the efficiency of alternative and species specific social foraging strategies using a high level visual interaction. This bioluminescent diversity may ultimately explain the evolutionary origin of species richness in *Etmopterus*. Obviously, this hypothesis is currently difficult to test, but improved possibilities both for direct observation in the deep-sea or in aquaria may be possible in the near future. Our phylogenetic analysis shows, that flank markings among (roughly) sympatric congeners may differ substantially, i.e. sympatric occurrence of clades V, VI, and VII (Fig. 1).

4.3. Phylogenetic implications

4.3.1. Trigonognathus

Clade I includes only a single extant species, *Trigonognathus kabeyai*. Shirai's analyses (1992) reveal *Trigonognathus* to be sister of *Aculeola* and *Centroscyllium*. Our combined dataset conversely identifies *Trigonognathus* well supported as sister genus to *Etmopterus* whereas the analyses of the nuclear RAG1 alone supports Shirai's hypothesis (Shirai, 1992) (Fig. 3). Morphological evidence does not favour either topology (Adnet et al., 2006; Shirai, 1992). Currently, only more nuclear data can reveal, whether alternative topologies favoured by our datasets are due to unambigous cytonuclear discordance or due to insufficient nuclear character sampling. Osteological and myological autapomorphies as identified by Shirai (1992) for *Trigonognathus* (Table 5) are numerous and are mapped on Fig. 1.

4.3.2. Placement of Aculeola, Centroscyllium and Miroscyllium sheikoi

Our molecular analyses confirm Shirai and Nakaya's (1990b) as well as Shirai's (1992) analysis and place *Aculeola* and *Centroscyllium* as sistertaxa to each other and both as sister taxon to *Etmopterus*. In contrast to their morphological analysis, our results show *Miroscyllium* (clade IV) to belong to the *E. lucifer* clade rendering *Etmopterus* paraphyletic with respect to *Miroscyllium*. Shirai and Nakaya (1990b) established the genus *Miroscyllium* for *Centroscyllium sheikoi* based on the mosaic morphological characterset of *Etmopterus* and *Centroscyllium*, i.e. a number of synapomorphies, a *Centroscyllium*-dentition of adults and flank markings as in *Etmopterus*. However, since subadult specimens of *M. sheikoi* show a dentition similar to that of *Etmopterus*, the adult dentition is interpretable as a *Centroscyllium*-convergent dentition secondarily derived from an *Etmopterus* dentition, and ontogenetically is not necessarily contradicting a placement of *M. sheikoi* within *Etmopterus*. Further, monophyly of *Etmopterus* and *Miroscyllium* is morphologically evidenced by an apparently synapomorphic short eyestalk (Shirai, 1992). Consequently, *Miroscyllium sheikoi* should be transferred to *Etmopterus*. However, its flank mark shape indicates a closer relationship between *Miroscyllium* and clade VII, rather than between *Miroscyllium* and clade V (as in our study).

4.3.3. Phylogenetic structure within Etmopterus

Within *Etmopterus*, we identified six monophyla including *Miroscyllium*. Those six clades are partitioned into two major monophyla, one comprising the *E. spinax* clade (II) and the *E. gracilispinis* clade (III), and the other one comprising *Miroscyllium*, two sisterclades within the major *E. lucifer* clade and *E. pusillus* clade (Fig. 1). In Shirai's analysis (1992) the first major monophylum (*E. spinax* and *E. gracilispinis* major clade) is morphologically supported (Table 5), but not all taxa analysed herein were represented in their dataset, i.e. morphological evidence needs to be substantiated with increased taxon sampling. There is currently no morphological support for our second major monophylum (clades IV–VII).

Clade II comprises the *E. spinax* clade, which had not been identified before. This group represents a quite recently evolved and diverse clade. Members of this group are distributed worldwide from subantarctic and – arctic zones to the tropics. Unfortunately, diagnostic morphological characters for the *E. spinax* clade are difficult to identify. External morphological characters traditionally used for species identification display much variation ranging from conspicuous flank markings with thin anterior and short and thick posterior branches (e.g. *E. granulosus, E. spinax*) to complete lack of flank markings (*E. princeps*), fine bristle-like hooked denticles irregularly arranged (*E. unicolor, E. spinax*) to rough textured denticles partially defined in rows (*E. granulosus*). More detailed morphological analyses have to be conducted to clearly separate species forming identified subclades within this group. The *E. spinax* clade is further partitioned into five well supported subclades. Here, *E. dianthus* is the sister taxon to a clade comprising the remaining five species (Supplementary Material 2). Differentiation within *E. granulosus* and *E. baxteri* from diverse locations appears to be recent and not unambiguous with regard to species assignment, i.e. with our limited sample the question of paraphyly of *E. baxteri* cannot be resolved but is subject to an ongoing study. Surprisingly, specimens included in our analyses identified as *E. unicolor* and *Etmopterus* sp. B are not monophyletic, suggesting that *E. unicolor* from close to the type locality in North East Pacific (Japan), is specifically distinct from *Etmopterus* sp. B (Last and Stevens, 1994) – specimens from New Caledonia. This contradicts recent morphological analyses (Yano, 1997), which had suggested conspecificity of specimens of *E. unicolor* with *Etmopterus* sp. B from southern Australia which was subsequently accepted in current literature (Last and Stevens, 2009). Specimens of *E.* cf. *granulosus* (Duhamel et al., 2005) from the Kerguelen Plateau form another subclade within clade II which is sister taxon to the *Etmopterus* sp. B subclade including specimens from New Zealand. This suggests that this undescribed species is wide spread throughout the Southern Hemisphere (NS, pers. obs.). This species is similar to *E. unicolor* and *Etmopterus* sp. B (shape and arrangement of dermal denticles) and *E. granulosus* (similar flank markings) suggesting these three species as cryptic species. It is most probably closely related to *E. litvinovi* (Kotlyar, 1990) and to another undescribed species from South Africa, *Etmopterus* sp. (Bass et al., 1986). This species will be described in a separate publication.

The four species of our *E. gracilispinis* clade (clade III) are confined to the Atlantic Ocean (incl. the Carribean) and southern Africa (*E. gracilispinis*) – a pattern of restricted endemism contrasting with the wide distribution range of the *E. spinax* clade (II). Shared external morphological characters within this group are hook-like denticles, never forming rows and flank markings displaying a short posterior (except *E. polli* and *E. robinsi*) but conspicuous anterior branch with a thinning of the dark area accumulating photophores at the basis of the marking (Table 5). According to these

characters, the rare Caribbean *E. perryi* belongs to this group, too (NS, pers. obs.). A remarkable aspect of this small marine elasmobranch species-flock is, that the intragroup heterogeneity of biolumiscent flank mark shapes is conspicuously larger than in other more widely distributed clades. Possibly, this diversity indicates that species recognition through diversification of flank marks helped establishing reproductive isolation among diverging tropical Atlantic Etmopteridae (see also Section 4.2).

Clades IV (*Miroscyllium*), V and VI represent a monophylum, which we name *E. lucifer* clade, because it comprises most species of the "*E. lucifer* species group" as defined by Yamakawa et al. (1986). However, our results partially contradict, because *E. granulosus* appears not to be a member of the *E. lucifer* clade and *Miroscyllium sheikoi* is a member of it. Yamakawa et al. (1986) diagnosed the group using the arrangement of dermal denticles in longitudinal rows along the flanks and included seven nominal species in this group: *E. lucifer, E. villosus, E. brachyurus, E. bullisi, E. abernethyi* (synonym of *E. lucifer* according to Last and Stevens, 1994), *E. molleri* and *E. granulosus*. In recent years, five newly described species were assigned to the "*E. lucifer* species group" (*E. burgessi* (Schaaf da Silva and Ebert, 2006), *E. decacuspidatus* (Chan, 1966), *E. dislineatus, E. evansi* (Last et al., 2002), and *E. pycnolepis* (Kotlyar, 1990)). Using flank mark shapes as potentially diagnostic characters instead of longitudinal rows of dermal denticles as diagnostic character for the *E. lucifer* clade, we find increased consistency of molecular results and morphology. Then, the *E. lucifer* clade is predominantly characterized by flank markings displaying conspicuous anterior and posterior branches, which are similar to those of *E. lucifer* (Yamakawa et al., 1986; Last et al., 2002; Schaaf da Silva and Ebert, 2006). This character would be suitable to identify all members of the molecularly identified *E. lucifer* clade except *M. sheikoi*. Based on results of this study, we remove *E. granulosus* from the traditional "*E. lucifer* species group" (Yamakawa et al., 1986), as it does not share the aforementioned flank mark characteristics and simultaneously is placed with the *E. spinax* clade using molecular characters. Nevertheless, we suggest to test the intrageneric placement of *M. sheikoi* along with the evolution of flank marks within *Etmopterus* using additional nuclear markers from several genomic regions. In summary, we suggest to re-define the "*E. lucifer* species group" as *E. lucifer* clade to comprise *E. brachyurus, E. bullisi, E. burgessi, E. decacuspidatus, E. dislineatus, E. evansi, E. lucifer, E. molleri, E. pycnolepis*, and possibly *M. sheikoi*.

Clade VII is herein referred to as the *E. pusillus* clade. Morphological analyses had identified an "*E. pusillus* species group" mainly characterized by conical, block-like dermal denticles (Shirai and Tachikawa, 1993). However, their analysis included only *E. bigelowi* and *E. pusillus*, which indeed form a monophyletic subclade with the *E. pusillus* clade. Here, we include in an *E. pusillus* clade species, which were previously included into a tentative "*E. splendidus* species group" namely *E. pseudosqualiolus* and *E. fusus* (Last et al., 2002). These do not share the conical denticles of *E. bigelowi* and *E. pusillus* but exhibit hook-like denticles in rows (Last et al., 2002). In summary, all species of our molecularly defined *E. pusillus* clade cannot be characterized by a uniform shape of denticles but by a very similar shape of flank markings which are characterised by an high and elongated anterior branch and no or only slightly visible posterior branches (Table 5). Our analyses did not include *E. carteri*, a dwarf species very similar to *E. pseudosqualiolus*. Images of the holotype of this rare species, reveal not only a similar body shape but also flank markings as in *E. pseudosqualiolus* (NS, pers. obs.). We therefore tentatively place this taxon with the *E. pusillus* clade.

Acknowledgments

Appendix A. Supplementary data

Supplementary data associated with this article can be found, in the online version, at doi:10.1016/j.ympev.2010.04.042.

References

Adnet, S., 2006. Two new selachian associations (Elasmobranchii, Neoselachii) from the Middle Eocene of Landes (south–west of France). Implication for the knowledge of deep-water selachian communities. Palaeo Ichthyologica 10, 5–128.

Adnet, S., Cappetta, H., 2001. A palaeontological and phylogenetical analysis of squaliform sharks (Chondrichthyes: Squaliformes) based on dental characters. Lethaia 34, 234–248.

Adnet, S., Cappetta, H., Nakaya, K., 2006. Dentition of etmopterid shark *Miroscyllium* (Squaliformes) with comments on the fossil record of Lantern Sharks. Cybium 30 (4), 305–312.

Adnet, S., Cappetta, H., Reynders, J., 2008. Contribution of Eocene sharks and rays from southern France to the history of deep-sea selachians. Acta Geol. Pol. 58 (2), 257–260.

Alegret, L., Cruz, L.E., Fenero, R., Molina, E., Ortiz, S., Thomas, E., 2008. Effects of the Oligocene climatic events on the formainiferal record from Fuente Caldera section (Spain, western Tethys). Palaeogeogr. Palaeolocl. 269, 94–102.

Bass, A.J., Compagno, L.J.V., Heemstra, P.C., 1986. Squalidae. In: Smith, M.M., Heemstra, P.C. (Eds.), Smith's Sea Fishes. Springer Verlag, Berlin, pp. 49–62.

Benton, M.J., Donoghue, P.C.J., 2007. Paleontological evidence to date the tree of life. Mol. Biol. Evol. 24 (1), 26–53.

Cadenat, J., Blache, J., 1981. Requins de Mediterranee et d'Atlantique (plus particulierement de la Coze occidentale d'Afrique). Faune Trop. 21, 330.

Cappetta, H., 1987. Les sélaciens du Crétacé supérieur du Liban. I. Requins. Palaeontographica A 168, 69–229.

Cappetta, H., Adnet, S., 2001. Discovery of the recent genus *Trigonognathus* (Squaliformes: Etmopteridae) in the Lutetian of Landes (southwestern France). Remarks on the teeth of the recent species *Trigonognathus* kabeyai. Paläontol. Z. 74 (4), 575–581.

Cappetta, H., Siverson, M., 2001. A skate in the lowermost Maastrichtian of southern Sweden. Palaeontology 44, 431–445.

Carvalho, M.R., de Maisey, J.G., 1996. Phylogenetic relationships of the Late Jurassic shark *Protospinax* Woodward 1919 (Chondrichthyes: Elasmobranchii). In: Arratia, G., Viohl, G. (Eds.), Mesozoic Fishes – Systematics and Paleoecology. Verlag Pfeil, München, pp. 9–46.

Chan, W.L., 1966. New Sharks from the South China Sea. J. Zool. 148, 218–237.

Cigala Fulgosi, F., 1986. A deep-water elasmobranch fauna from the Pliocene outcropping (North Italy). In: Proceedings of the 2nd Conference of Indopacific fishes. Uyeno, T., Arai, R., Taniuchi, T., Matsuura, K. (Eds.). Ichthyological Society of Japan, pp. 133–139.

Claes, J.M., Mallefet, J., 2008. Early development of bioluminescence suggests camouflage by counter-illumination in the velvet belly lantern shark *Etmopterus spinax* (Squaloidea: Etmopteridae). J. Fish Biol. 73, 1337–1350.

Claes, J.M., Mallefet, J., 2009. Ontogeny of photophore pattern in the velvet belly lantern shark, *Etmopterus spinax*. Zoology. doi:10.1016/j.zool.2009.02.003.

Coelho, R., Erzini, K., 2008a. Identification of deep-water Lantern Sharks (Chondrichthyes: Etmopteridae) using morphometric data and multivariate analysis. J. Mar. Biol. Assoc. UK 88 (1), 199–204.

Coelho, R., Erzini, K., 2008b. Life history of a wide-ranging deep-water Lantern Shark in the north–east Atlantic, *Etmopterus spinax* (Chondrichthyes: Etmopteridae), with implications for conservation. J. Fish Biol. 73, 1419–1443.

Compagno, L.J.V., 1973. Interrelationships of living elasmobranchs. In: Greenwood, P.H. et al. (Eds.), Interrelationships of Fishes. Academic Press, London, pp. 15–61.

Compagno, L.J.V., 1977. Phyletic relationships of living sharks and rays. Am. Zool. 17, 303–322.

Compagno, L.J.V., 1984. FAO species catalogue. Vol. 4. Sharks of the world. An annotated and illustrated catalogue of sharks species known to date. Part 1. Hexanchiformes to Lamniformes. FAO Fish Synop. vol. 1254(1), pp. 1–249.

Compagno, L.J.V., Dando, M., Fowler, S., 2005. A Field Guide to the Sharks of the World. Collins, London. pp. 1–368.

Dalebout, M.L., Steel, D., Baker, S., 2008. Phyogeny of the beaked whale Genus Mesoplodon (Ziphiidae: Cetacea) revealed by nuclear introns: implications for the evolution of male tusks. Syst. Biol. 57 (6), 857–875.

Drummond, A.J., Ho, S., Philipps, M., Rambaut, A., 2006. Relaxed phylogenetics and dating with confidence. PloS Biol. 4, 88.

Drummond, A.J., Rambaut, A., 2007. BEAST: Bayesian evolutionary analysis by sampling trees. BMC Evol. Biol. 7, 214.

Duhamel, G., Gasco, N., Davaine, P., 2005. Poissons des iles Kerguelen et Crozet. Guide regional de l'ocean Austral. Museum national d'Histoire naturelle, Paris. pp. 62–74.

Edgar, R.C., 2004. MUSCLE: multiple sequence alignment with high accuracy and high throughput. Nucleic Acids Res. 32 (5), 1792–1797.

Eldrett, J.S., Greenwood, D.R., Harding, I.C., Huber, M., 2009. Increased seasonality through the Eocene to Oligocene transition in northern high latitudes. Nature 459, 969–973.

Eriksson T., 2007. r8s bootstrap kit. Published by the author.

Felsenstein, J., 2005. PHYLIP. Phylogeny Inference Package (Version 3.6.7). Distributed by the author. Department of Genome Sciences, University of Washington, Seattle, USA.

Hall, T.A., 1999. BioEdit: a user-friendly biological sequence alignment editor and analysis program for Windows 95/98/NT. Nucl. Acids. Symp. Ser. 41, 95–98.

Hardman, M., Hardman, L.M., 2008. The relative influence of body size and paleoclimatic change as explanatory variables influencing lineage diversification rate: an evolutionary analysis of bullhead catfishes (Siluriformes: Ictaluridae). Syst. Biol. 57 (1), 116–130.

Hubbs, C.L., Iwai, T., Matsubara, K., 1967. External and internal characters, horizontal and vertical distribution, luminescence, and food of the dwarf pelagic shark *Euprotomicrus bispinatus*. Bull. Scripps Inst. Oceanogr. Univ. Calif. 10, 1–64.

Huelsenbeck, J.P., Ronquist, F., 2001. MRBAYES: Bayesian inference of phylogenetic trees. Bioinformatics 17, 754–755.

Iglésias, S.P., Lecointre, G., Sellos, D.Y., 2005. Extensive paraphyllis within sharks of the order Carcharhiniformes inferred from nuclear and mitochondrial genes. Mol. Phylogenet. Evol. 34, 569–583.

Klimpel, S., Palm, H.W., Seehagen, A., 2003. Metazoan parasites, food composition of juvenile *Etmopterus spinax* (L. 1758) (Dalatiidae, Squaliformes) from the Norwegian Deep. Parasitol. Res. 89, 245–251.

Kotlyar, A.N., 1990. Dogfish Sharks of the genus *Etmopterus* Rafinesque from the Nazca and Sala y Gomez Submarine Ridges. Trudy Instituta Okeanologii 125, 127–147.

Kriwet, J., Benton, M., 2004. Neoselachian (Chondrichthyes, Elasmobranchii) diversity across the K/T boundary. Palaeogeogr. Palaeocl. 214, 181–194.

Kriwet, J., Klug, S., 2004. Late Jurassic Selachians (Chondrichthyes: Elasmobranchii) from Southern Germany: re-evaluation on taxonomy and diversity. Zitteliana A44, 67–95.

Kriwet, J., Klug, S., 2010. Timing of deep-sea adaptation in dog-fish sharks: insights from a supertree of extinct and extant taxa. Zoologica Scripta, doi:10.1111/j.1463-6409.2010.00427.x.

Last, P.R., Burgess, G.H., Seret, B., 2002. Description of six new species of Lantern-Sharks of the genus *Etmopterus* (Squaloidea: Etmopteridae) from the Australasian region. Cybium 26, 203–223.

Last, P.R., Stevens, J.D., 1994. Sharks and Rays of Australia. CSIRO Australia, pp. 1–513.

Last, P.R., Stevens, J.D., 2009. Sharks and Rays of Australia, 2nd ed. Harvard University Press, Cambridge, pp. 1–554.

Lear, C.H., Bailey, T.R., Pearson, P.N., Coxall, H.K., Rosenthal, Y., 2008. Cooling and ice growth across the Eocene–Oligocene transition. Geology 36, 251–254.

Ledoux, J.-C., 1972. Les Squalidae (Euselachii) miocenes des environs d'Avignon (Vaucluse). Doc. Lab. Geol. Fac. Sci. Lyon, Notes Mem 52, 133–175.

Lindberg, D.R., Pyenson, N.D., 2007. Things that go bump in the night: evolutionary interactions between cephalopods and cetaceans in the tertiary. Lethaia 40, 335–343.

Macpherson, E., 1980. Régime alimentaire de Galeus melastomus Rafinesque, 1810, *Etmopterus spinax* (L., 1758) et Schymnorhinus licha (Bonnaterre 1788) en Méditerranée occidentale. Vie et Milieu 30, 139–148.

Maisey, J.G., Naylor, G.J.P., Ward, D.J., 2004. Mesozoic elasmobranchs, neoselachian phylogeny and the rise of modern elasmobranch diversity. In: Arratia, G., Tintori, A. (Eds.), Mesozoic Fishes 3-Systematics. Palaeoenvironments and Biodiversity. Verlag Dr. Friedrich Pfeil, Munich, pp. 17–56.

Misof, B., Misof, K., 2009. A Monte Carlo approach successfully identifies randomness of multiple sequence alignments: a more objective means of data exclusion. Syst. Biol. 58 (1), 21–34.

Müller, A., Schöllmann, L., 1989. Neue Selachier (Neoselachii, Squalomorphii) aus dem Campanium Westfalens (NW-Deutschland). Neues Jahrb. Geol. Palaeontol., Abh. 178, 1–35.

Naylor, G.J.P., Ryburn, J.A., Fedrigo, O., Lopez, A., 2005. Phylogenetic relationships among the major lineages of modern elasmobranchs. In: Hamlett, W.C. (Ed.), Reproductive Biology and Phylogeny of Chondrichthyes; Sharks. Batoids and Chimaeras. Science Publishers Inc., Enfield, pp. 1–25.

Neiva, J., Coelho, R., Erzini, K., 2006. Feeding habits of the velvet belly lanternshark *Etmopterus spinax* (Chondrichthyes: Etmopteridae) off the Algarve, southern Portugal. J. Mar. Biol. Assoc. UK 86, 835–841.

Nylander, J.A.A., Ronquist, F., Huelsenbeck, J.P., Nieves-Aldrey, J.L., 2004. Bayesian phylogenetic analysis of combined data. Syst. Biol. 53 (1), 47–67.

Pattengale, N.D., Alipour, M., Bininda-Edmonds, O.R.P., Moret, B.M.E., Stamatakis, A., 2009. How many Bootstrap replicates are necessary? Presented at: International Conference on Research in Computers. Molecular Biology RECOMB. Tucson. In: Proceedings of the 13th International Conference on Research in Computational Molecular Biology RECOMB. 2009, Springer 2009. Lecture Notes in Computer Science. Online Pre-print: http://lcbb.epfl.ch/bootstrapping.pdf.

Reif, W.E., 1985. Functions of scales and photophores in Mesopelagic Luminescent Sharks. Acta Zool.-Stockholm 66 (2), 111–118.

Sanderson, M.J., 2002. Estimating absolute rates of molecular evolution and divergence times: a penalized likelihood approach. Mol. Biol. Evol. 19, 101–109.

Sanderson, M.J., 2003. R8s: inferring absolute rates of molecular evolution and divergence times in the absence of a molecular clock. Bioinformatics 19, 301–302.

Schaaf da Silva, J.A., Ebert, D., 2006. *Etmopterus burgessi* sp. Nov., a new species of lantern shark (Squaliformes: Etmopteridae) from Taiwan. Zootaxa 1273, 53–64.

Siverson, M., 1993. Maastrichthian squaloid sharks from southern Sweden. Palaeontology 36 (1), 1–19.

Shirai, S., Nakaya, K., 1990a. A new squalid species of the genus *Centroscyllium* from the Emperor Seamount Chain. Jpn. J. Ichthyol. 36, 391–398.

Shirai, S., Nakaya, K., 1990b. Interrelationships of the Etmopteridae (Chondrichtyes, Squaliformes). In: Pratt, H.L. JR., Gruber, S.H., Taniuchi, T. (Eds.). Elasmobranchs as Living Resources: Advances in Biology, Ecology, Systematics and the status of the fisheries. NOAA Technical report 90, pp. 347–356.

Shirai, S., 1992. Squalean Phylogeny and Related Taxa. Hokkaido University Press. pp. 1–151.

Shirai, S., Tachikawa, H., 1993. Taxonomic resolution of the *Etmopterus pusillus* species group (Elasmobranchii, Etmopteridae) with description of *E. bigelowi*, n. sp.. Copeia 2, 483–495.

Springer, S., 1967. Social organization of shark populations. In: Gilbert, P.W., Mathewson, R.F., Rall, D.P. (Eds.), Sharks Skates and Rays. Johns Hopkins University Press, Baltimore, pp. 503–531.

Springer, S., Burgess, G.H., 1985. Two New Dwarf Dogsharks (*Etmopterus*, Squalidae), found off the Carribean Coast of Colombia. Copeia 3, 584–591.

Stamatakis, A., 2006. RAxML-VI-HPC: maximum Likelihood-based phylogenetic analyses with thousands of taxa and mixed models. Bioinformatics 22 (21), 2688–2690.

Stanley, M., 2009. Earth system history. In: Raymond, V., Clench, W., Thorne, A. (Eds.). W.H. Freeman and Company, New York, USA. pp. 1–549.

Straube, N., Schliewen, U., Kriwet, J., 2008. Dental Structure of the Giant lantern shark, *Etmopterus baxteri* (Chondrichthyes: Squaliformes) and its taxonomic implications. Environ. Biol. Fish. 82, 133–141.

Swofford, D.L., 2003. PAUP*. Phylogenetic analysis Uing Parsimony (*and Other Methods). Version 4. Sinauer Associates, Sunderland, Massachusetts.

Thies, D., Müller, A., 1993. A neoselachian fauna (Vertebrata, Pisces) from the Late Cretaceous (Campanian) of Höver, near Hannover (NW, Germany). Paläontol. Z. 67, 89–107.

Tracer, v1.4. (http://beast.bio.ed.ac.uk/tracer).

Türkay, M., 2002. Die Tiefsee. In: Hofrichter (Ed.), Das Mittelmeer. Fauna, Flora, Ökologie. Band I: Allgemeiner Teil. Spektrum Akademischer Verlag Heidelberg, Berlin, pp. 416–423.

Underwood, C.J., Mitchell, S.F., 1999. Albian and Cenomanian selachian assemblages from north–east England. Spec. Pap. Palaeontol. 60, 9–56.

Venkatesh, B., Kirkness, E.F., Loh, Y.H., Halpern, A.L., Lee, A.P. et al., 2007. Survey sequencing and comparative analysis of the elephant shark (Callorhinchus milii) genome. PLoS Biology 5(4), e 101. doi:10.1371/journal.pbio.0050101.

Ward, R.D., Zemlak, T.S., Innes, B.H., Last, P.R., Hebert, D.N., 2005. DNA barcoding Australia's fish species. Phil. Trans. R. Soc. Lond. B 360, 1847–1857.

Ward, R.D., Holmes, B.A., Zemlak, T.S., Smith, P.J., 2007. Part 12-DNA barcoding discriminates spurdogs of the genus Squalus. In: Last, P.R., White, W.T., Pogonoski J.J. (Eds.), Descriptions of new dogfishes of the genus Squalus (Squaloidea: Squalidae). CSIRO Marine and Atmospheric Research Paper No. 14, pp. 114–130.

Widder, E., 1998. A predatory use of counter illumination by the squaloid shark, Isistius brasiliensis. Environ. Biol. Fish. 53, 267–273.

Yamakawa, T., Taniuchi, T., Nose, Y., 1986. Review of the *Etmopterus lucifer* Group (Squalidae) in Japan. In: Uyeno, T., Arai, R., Taniuchi, T., Matsuura, K. (Eds.), Indo-Pacific Fish Biology: Proceedings of the Second International Conference on Indo-Pacific fishes. Ichthyological Society of Japan, Tokyo, pp. 197–207.

Yano, K., 1997. First record of the brown lantern shark, *Etmopterus unicolor*, from the waters around New Zealand, and comparison with the southern lantern shark, *E. Ganulosus*. Ichthyol. Res. 44 (1), 61–72.